IGF26 - 26th International Conference on Fracture and Structural Integrity

Effect of remaining ligament on fatigue crack growth

Joel Jesus[a]*, DM Neto[a], RF Fernandes[a], MF Borges[a], FV Antunes[a], ER Sérgio[a]

[a]Univ Coimbra, Centre for Mechanical Engineering, Materials and Processes (CEMMPRE), Department of Mechanical Engineering, Rua Luís Reis Santos 3030-788 Coimbra, Portugal

Abstract

Fatigue crack growth (FCG) has been studied assuming that ΔK_{eff} is the crack driving force. However, the effect of crack ligament on FCG rate is not clear. Experimental-numerical work was developed in the 18Ni300 maraging steel considering different load blocks with the same initial ΔK. No effect of crack ligament was observed experimentally, which was explained by the inexistence of crack closure effects. In the numerical work transient effects were observed for the plane stress state, which disappear for the plane strain state and some effect of crack ligament was found. In both cases this was attributed to crack closure phenomenon.

Keywords: Fatigue crack growth; 18Ni300; Crack cloure; Crack ligament

1. Introduction

da/dN-ΔK curves have been widely used to study fatigue crack growth (FCG) in metallic materials. However, these empirical models are not able to explain the effect of stress ratio or variable amplitude loading. Therefore, the concept of crack closure was successfully introduced by Elber (1970). Crack closure seems to be able to explain the influence of mean stress in both regimes I and II of crack propagation (Borrego, 2001), the transient crack growth behaviour following overloads (Borrego, 2003), the growth rate of short cracks (Rao, 1988), and the effect of thickness on fatigue crack growth (Bao, 1998; Costa, 1998), among other aspects. In a previous study it was found

* Corresponding author. Tel.: 00351 239 790722; fax: 00351 239 790701.
  E-mail address: fernando.ventura@dem.uc.pt

that crack closure is, in fact, the only responsible for the typical behaviour of FCG observed after an overload (Neto, 2021).

According to Elber's understanding of crack closure, as the crack propagates due to cyclic loading, a residual plastic wake is formed. The deformed material acts as a wedge behind the crack tip and the contact of fracture surfaces is forced by the elastically deformed material. The load at which the contact of crack flanks disappears is called crack opening load, K_{open}. However, it is obvious that the remaining ligament ahead of crack tip has no influence on crack closure and therefore on FCG rate. In fact, Gonzaléz *et al.* (2020) observed a decrease of crack closure level while da/dN was constant in experimental tests in 6351-T6 aluminium alloy and 1020 steel, made at constant ΔK and K_{max}.

Therefore, experimental work was developed here to obtain da/dN-ΔK curves for three load blocks in a CT specimen, each occupying 3 mm of crack propagation. The same ΔK was considered at the beginning of each load block. The material studied was the 18Ni300 steel obtained by additive manufacturing. A numerical study was developed replicating the experimental work in order to understand the fundamental mechanisms behind the trends observed.

2. Experimental work

2.1. Experimental procedure

FCG tests were performed in mode I loading using compact tension (CT) specimens with a width W=36 mm and a thickness of 6 mm, following ASTM E647 (2016) recommendations. The specimens, made of 18Ni300 maraging steel, were obtained by Laser powder bed fusion (LPBF). The machine used a high-power laser type Nd: YAG with a maximum power of 400 W in continuous wave mode, a wavelength of 1064 nm and 0.04 mm of laser beam diameter. The 18Ni300 powder used to produce the samples had an average particle size of 40 μm, giving layers of 30 μm thickness. These sample layers were deposited in planes perpendicular to the loading direction.

The FCGR tests were carried out at room temperature using a 10 kN capacity Instron EletroPuls E10000 machine, at constant amplitude load with a loading frequency of 10 Hz. Table 1 presents the load conditions applied during the test. Three load blocks were considered, keeping the maximum load constant. After 3 mm of crack propagation, the minimum load was increased in order to have the same ΔK at the beginning of the load block.

The crack length was measured every 0.1 mm of crack propagation using a travelling microscope (45x) with an accuracy of 10 μm. Crack growth rates under constant amplitude loading were determined by the incremental polynomial method using five consecutive points of a-N curves. Crack closure was measured using the load-displacement data acquired at 0.1 mm of crack length increments using an Allied Vision Stingray camera (20+75 mm) to take images. These images were subsequently processed by digital image correlation (DIC) with the GOM correlate software. The crack opening load was estimated using the maximization of correlation coefficient.

Table 1. Parameters of experimental test.

Block	a_{min} [mm]	a_{max} [mm]	F_{max} [N]	F_{min} [N]	R	ΔK_0 [MPa.m$^{0.5}$]	$K_{max,0}$ [MPa.m$^{0.5}$]
1	14.0	17.0	3026.3	151.3	0.05	18.1	19.1
2	17.0	20.0	3026.3	724.0	0.24	18.1	23.8
3	20.0	23.0	3026.3	1260.0	0.42	18.1	31.1

2.2. Experimental results

Figure 1a plots the da/dN-ΔK curves obtained for the three load blocks. There is no significant influence of load block, which indicates that the crack ligament does not seem to have a significant influence on FCG rate, at least for the 18Ni300 steel. Additionally, the increase of da/dN with crack length is not evident, which was unexpected. The transition between load blocks does not produce transient effects, which could be expected since the crack closure phenomenon does not seem to affect significantly this material (Antunes, 2019). The load blocks are not evident on the fracture surface which indicates than marking cannot be done fixing the maximum load.

Figure 1b plots previous results obtained for constant amplitude loading considering two load ratios (R=0.05 and R=0.3) (Antunes, 2019). There is no significant effect of stress ratio, which once again indicates that crack closure is not relevant. The increment of da/dN with ΔK is now evident, and the results obtained for the load blocks are coincident with the constant amplitude results.
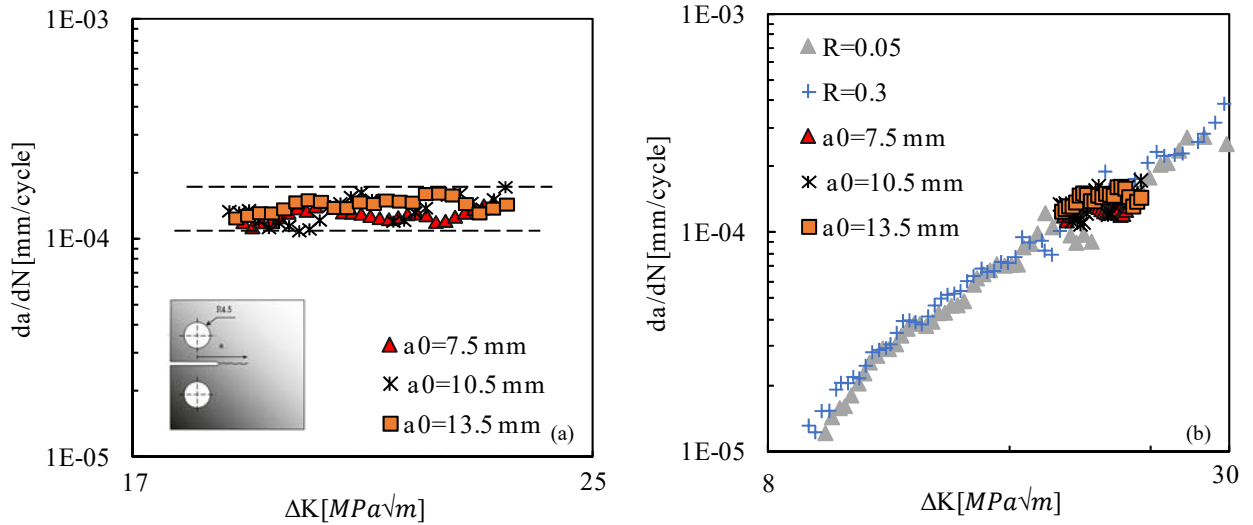

Fig. 1. da/dN-ΔK curves. (a) Results for the load block. (b) Comparison with previous results for constant amplitude loading (Antunes, 2019).
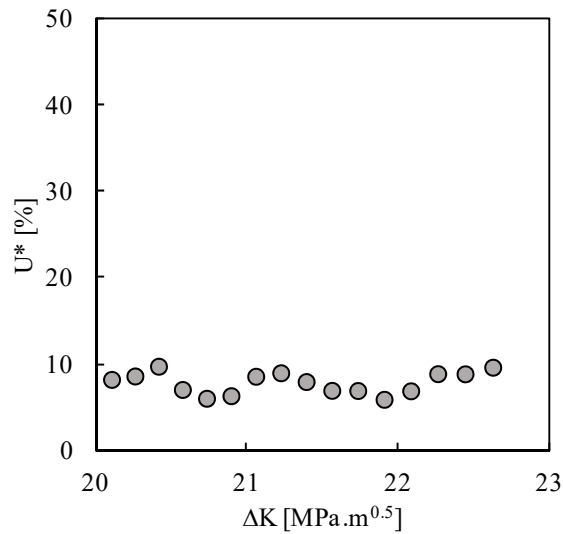

Fig. 2. Crack closure level for the first load block (R=0.05).

Figure 2 plots the crack closure level obtained for the first load block, quantified by U*, which is the percentage of load range during which the crack is closed:

$$U^* = \frac{F_{open} - F_{min}}{F_{max} - F_{min}} \times 100 \qquad (1)$$

where F_{open} is the opening load, F_{max} is the maximum load and F_{min} is the minimum load. The values present some oscillation, having an average value of 8.1 %. This is a relatively low value, which indicates plane strain state is dominant. No crack closure was obtained for the second and third load blocks, i.e., $U^*=0$. This could be expected since the increase of stress ratio (see Table 1) promotes the reduction of crack closure phenomenon.

3. Numerical work

3.1. Numerical model

1/4 of the C(T) specimen with W=36 mm was modeled numerically considering adequate boundary conditions. A pure plane stress state was simulated by assuming a small thickness equal to 0.1 mm, while plane strain state was simulated imposing out-of-plane constraints. The maximum and minimum values of the remote load were defined considering the experimental loads listed in Table1. The maximum load was kept constant while the minimum load increased with load block in order to have the same ΔK at the beginning of the different load blocks, as presented in Table 2.

Table 2. Parameters of numerical tests.

Block	a_{min} [mm]	a_{max} [mm]	F_{max} [N]	F_{min} [N]	R	ΔK_0 [MPa.m$^{0.5}$]	$K_{max,0}$ [MPa.m$^{0.5}$]
1	14.0	17.3	50.439	2.522	0.05	17.9	18.9
2	17.3	20.0	50.439	12.067	0.24	18.4	24.1
3	20.0	23.0	50.439	21	0.42	18.0	30.8

The finite element mesh of the CT specimen comprised 7142 linear isoparametric elements and 14606 nodes, with two main regions: (i) an ultra-refined mesh near the crack tip, composed of elements with 8×8 µm side; (ii) a coarser mesh in the remaining specimen, to reduce the computational overhead. Only one layer of elements through-thickness was used. The crack propagation occurs at the minimum load, by successive debonding of both crack front nodes over the thickness. The numerical simulations were performed using the DD3IMP (Deep-Drawing 3D IMPlicit) in-house code, originally developed to model deep-drawing processes (Menezes, 2000). The evolution of the deformation is modeled by an updated Lagrangian scheme, assuming a hypoelastic-plastic material model. The contact between crack flanks is modeled considering a rigid plane surface aligned with the crack symmetry plane. A master–slave algorithm is used; an augmented Lagrangian approach is used for the contact problem treatment. An elastic-plastic model was used: the isotropic elastic behaviour is modeled by the generalised Hooke's law; the plastic behaviour is described by the von Mises yield criterion coupled with a mixed isotropic-kinematic hardening law, under an associated flow rule. The elastic-plastic parameters are shown in Table 3.

Table 3. Parameters of elastic-plastic model.

	Hooke's law parameters		Isotropic hardening (Swift)			Kinematic hardening (Armstrong-Frederick)	
Material	E	v	Y_0	C	n	C_X	X_{Sat}
	[GPa]	[-]	[MPa]	[MPa]	[-]	[-]	[MPa]
18Ni300	165	0.30	683.62	683.62	0	728.34	402.06

The FCG is modelled by nodal release, using the approach proposed by Ferreira *et al.* (2020). The crack propagation is uniform along the thickness, releasing simultaneously both crack front nodes. The nodal release occurs when the plastic strain at the crack tip achieves a critical value. Nevertheless, it is only performed when the load is minimum to avoid eventual convergence problems related with the high tensile stresses occurring at maximum load. Assuming that the damage accumulation is responsible for FCG, the total plastic strain accumulated during the entire cyclic loading is considered. Only a single material parameter is required for this fatigue crack growth criterion, which simplifies its usage. Accordingly, the critical value of plastic strain involved in this FCG

criterion was calibrated for this maraging steel in a previous work ($\Delta\varepsilon_p^c$), comparing experimental da/dN values with numerical predictions under plane stress conditions (Borges, 2020). In this study, the FCG rate (da/dN) is assessed through the ratio between the element size (8 μm) and the number of load cycles required to achieve the critical value of plastic strain at the crack tip.

3.2. Numerical results

Figure 3 compares results for two different load blocks. At the beginning of numerical simulation there is a transient regime resulting essentially from the formation of residual plastic wake needed to produce plasticity induced crack closure. Under plane stress state this transient extends over 130 μm for a_0=16.5 mm and over 180 μm for a_0=19.5 mm. For plane strain state this regime almost disappears, which indicates that there is no crack closure. The stable FCG rate is higher for the longer crack length, which indicates that there is an influence of crack length or remaining ligament on FCG rate. This influence may be associated with variations of crack closure. This effect of crack length on FCG rate is also observed for plane strain state but in a less extent. Note also that after stabilization there is a progressive increase of da/dN with crack length, which is associated with the increase of ΔK.

The decrease of load range produced by the increase of minimum load, as indicated in Table 2, produces a sudden decrease of FCG rate. For plane stress regime there a second transient regime extending over about 80 μm. In this regime, da/dN decreases to a minimum value and then increases progressively to the value of da/dN corresponding to the second load block. For plane strain, once again this transient regime is almost inexistent. But, after the transition there is a coincidence of FCG rate for the different remaining ligaments, which indicates that this parameter does not affect directly FCG rate.
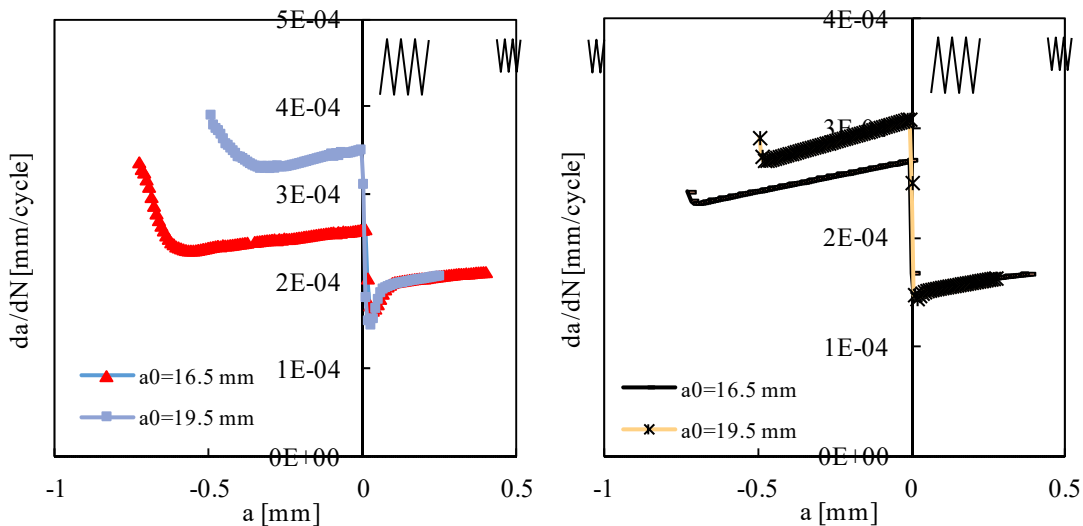

Fig. 3. Effect of crack length on FCG rate (a) Plane stress state. (b) Plane strain state.

Table 4 present the crack closure values predicted numerically using the contact status of the first node behind crack tip. The values were obtained at the beginning and end of each load block, after stabilization. U* is higher for lower stress ratios, increasing with ΔK, as could be expected. For plane strain state no crack closure was observed. The independence of da/dN observed in Figure 3 after the increase of stress ratio I explained by the elimination of crack closure.

Table 4. Crack closure level for plane stress state.

Block	a_{min} [mm]	a_{max} [mm]	F_{max} [N]	F_{min} [N]	R	a	ΔK [MPa.m$^{0.5}$]	U*
1	14.0	17.3	50.439	2.522	0.05	14.152	18.05113	9.09
1	14.0	17.3	50.439	2.522	0.05	17.26	22.92682	16.7
2	17.3	20.0	50.439	12.067	0.24	17.612	18.90365	0
2	17.3	20.0	50.439	12.067	0.24	20.004	23.43884	9.2
3	20.0	23.0	50.439	21	0.42	20.252	18.42356	0
3	20.0	23.0	50.439	21	0.42	22.94	24.70953	6

Figure 4 studies the effect of stress state on the trends observed. As already mentioned, the transients greatly depend on stress state. Under plane strain state, there is almost no transient effect, which is a consequence of the limited influence of crack closure. For plane stress state the initial decrease is due to progressive increase of crack closure level, until its stabilization. After the increase of minimum load there is a significant decrease of da/dN down to a minimum value, followed by a progressive increase to the stable value. This valley of da/dN-a curve is due to the influence of residual plastic wake of previous load range, which progressively disappears.
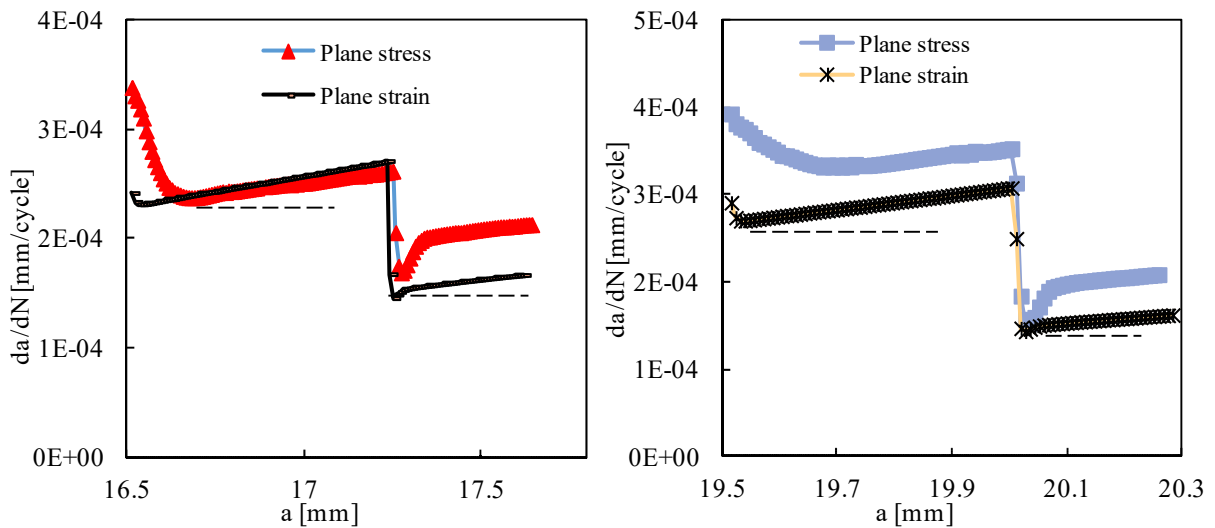
Fig. 4. Effect of stress state (a) a_0=16.5 mm. (b) a_0=19.5 mm.

4. Conclusions

A experimental-numerical study was developed to study the effect of remaining ligament on FCG rate. Three load blocks were considered with the same initial ΔK. No effect of crack ligament was observed experimentally, which was explained by the inexistence of crack closure effects. In the numerical work transient effects were observed for the plane stress state, which disappear for the plane strain state and some effect of crack ligament was found. In both cases this was attributed to crack closure phenomenon.

Acknowledgements

References

Antunes, F.V., Santos, L., Capela, C., Ferreira, J.M., Costa, J.D., Jesus, J., Prates, P., 2019. Fatigue Crack Growth in Maraging Steel obtained by Selective Laser Melting. Applied Science 9, 4412.

Bao, H. McEvily, A.J., 1998. On Plane Stress-Plane Strain Interactions in Fatigue Crack Growth. Int J Fatigue 20(6), 441-448.

Borges, M.F., Neto, D.M. Antunes, F.V., 2020. Numerical simulation of fatigue crack growth based on accumulated plastic strain. Theor Appl Fract Mech 108, 102676.

Borrego, L.F.P., 2001. Fatigue crack growth under variable amplitude loading in AlMgSi aluminium alloys. PhD thesis, University of Coimbra, Portugal.

Borrego, L.P., Ferreira, J.A.M., Pinho da Cruz, J.M., Costa, J.M., 2003. Evaluation of overload effects on fatigue crack growth and closure. Engng Fract Mech 70, 1379-1397.

Costa, J.D.M., Ferreira, J.A.M., 1998. Effect of Stress Ratio and Specimen Thickness on Fatigue Crack Growth of CK45 Steel. Theor Appl Fract Mech 30, 65-73.

Elber, W., 1970. Fatigue crack closure under cyclic tension. Engng Fract Mech 2, 37-45.

Ferreira, F.F.; Neto, D.M.; Jesus, J.S.; Prates, PA; Antunes, F.V., 2020. Numerical Prediction of the Fatigue Crack Growth Rate in SLM Ti-6Al-4V Based on Crack Tip Plastic Strain. Metals 10, 1133.

González, J.A.O., Castro, J., Meggiolaro, M.A., Gonzáles, G.L.G., Freire, J.L.F., 2020. Challenging the "ΔKeff is the driving force for fatigue crack growth" hypothesis, Int J Fatigue 136, 105577.

Menezes, L.F., Teodosiu, C., 2000. Three-Dimensional Numerical Simulation of the Deep-Drawing Process using Solid Finite Elements, J Mater Processing Technol 97, 100-106.

Neto, D.M., Borges, M.F., Antunes, F.V., Jesus, J., 2021. Mechanisms of fatigue crack growth in Ti-6Al-4V alloy subjected to single overloads, Theoretical and Applied Fracture Mechanics 114, 103024.

Rao, K.T.V., Yu, W., Ritchie, R.O., 1988. On the behaviour of small fatigue cracks in commercial aluminium lithium alloys. Engng Fract Mech 31(4), 623-635.